applied sciences

MDPI

Article

Assessment of the NO_2 Spatio-Temporal Variability over Thessaloniki, Greece, Using MAX-DOAS Measurements and Comparison with S5P/TROPOMI Observations

Dimitris Karagkiozidis [1,*], Maria-Elissavet Koukouli [1], Alkiviadis Bais [1], Dimitris Balis [1] and Paraskevi Tzoumaka [2]

[1] Laboratory of Atmospheric Physics, Aristotle University of Thessaloniki, 54124 Thessaloniki, Greece
[2] Municipality of Thessaloniki, Department of Environment, 54642 Thessaloniki, Greece
* Correspondence: dkaragki@auth.gr

Abstract: In this article, we investigate the spatio-temporal variability of tropospheric NO_2 Vertical Column Densities (VCDs) and surface concentrations that were retrieved using Multi-Axis Differential Optical Absorption Spectroscopy (MAX-DOAS) measurements over Thessaloniki, Greece, for the period June 2020 to November 2022. The MAX-DOAS system captures the NO_2 seasonal variability very well, reporting low concentrations during summer and higher concentrations in the winter, as well as the diurnal cycle with higher NO_2 amounts in the morning followed by a reduction towards noon. The "weekend effect" is evident, with approximately 30% lower NO_2 concentrations on the weekends compared to the working days. An excellent agreement is found with in situ data from a nearby air quality monitoring station with Pearson's correlation coefficients ranging between R = 0.90 and R = 0.99. The spatial variability is assessed by comparing the NO_2 concentrations at four azimuth viewing directions of the MAX-DOAS system. Despite the large variability due to short- and long-term temporal variations, higher NO_2 concentrations of up to 25% (statistically significant at the 95% confidence level) are reported for the azimuth that crosses the entire city center and an urban area compared to those pointing towards the sea. The MAX-DOAS tropospheric NO_2 columns are then compared to those measured by the TROPOspheric Monitoring Instrument (TROPOMI) on board the Sentinel-5P satellite. Despite the generally good correlation (R = 0.72 and R = 0.89 for the daily and monthly data, respectively), a clear underestimation of TROPOMI is found (approximately 55% in winter, 21% in spring and 40% during autumn and summer), mainly due to the much larger satellite footprint that provides a smoother perception of the NO_2 concentration, while the MAX-DOAS measurements are more affected by local emissions.

Keywords: MAX-DOAS; TROPOMI; tropospheric; NO_2; air quality; Thessaloniki

Citation: Karagkiozidis, D.; Koukouli, M.-E.; Bais, A.; Balis, D.; Tzoumaka, P. Assessment of the NO_2 Spatio-Temporal Variability over Thessaloniki, Greece, Using MAX-DOAS Measurements and Comparison with S5P/TROPOMI Observations. *Appl. Sci.* **2023**, *13*, 2641. https://doi.org/10.3390/app13042641

Academic Editor: Thomas Maggos

Received: 24 January 2023
Revised: 13 February 2023
Accepted: 15 February 2023
Published: 18 February 2023

1. Introduction

Atmospheric pollution and air quality are important environmental and research issues worldwide. On a global scale, nitrogen dioxide (NO_2) is considered a major tropospheric gaseous pollutant in most urban and industrial environments, strongly affecting air quality and human health [1]. NO_2 plays a key role in the photochemistry of the troposphere [2], acting as a precursor in the formation of tropospheric ozone (O_3) and, hence, it indirectly affects the radiative forcing of the atmosphere [3]. In the boundary layer, NO_2 is a short-lived pollutant that is mainly produced by the oxidation of nitrogen monoxide (NO), and it is emitted in the troposphere as a result of both natural and anthropogenic processes. The primary natural sources are soil emissions and lightning, while the main anthropogenic sources include biomass burning and fossil fuel combustion from domestic heating sources and motor vehicles [4,5]. Given the influence of NO_2 on atmospheric pollution and air quality, the importance for its accurate detection, the determination of its emission sources and the investigation of its spatio-temporal variability is self-evident.

Thus, continuous monitoring of NO_2 concentrations has been widely performed over the past few decades using both ground-based measurements and satellite observations. Over Thessaloniki, Greece, air quality monitoring and trace gas measurements are primarily performed by ground-based in situ instruments, with some of them reporting to the European Environmental Agency [6]. These continuous in situ measurements provide valuable information on various atmospheric pollutants (including NO_2) at fixed sampling stations, but their limited number does not allow a representative spatial coverage over the area of Thessaloniki. Furthermore, most of the stations have their sampling inlets installed close to the ground (a few meters above the surface) and are consequently mostly affected by local traffic emissions. Thus, these measurements are usually not representative of the average pollution levels in the local boundary layer and, moreover, they cannot provide information for the pollutants' vertical distribution.

Ground-based Multi Axis Differential Optical Absorption Spectroscopy (MAX-DOAS) is a remote sensing measurement technique for the detection of aerosols and trace gases in the troposphere that represents a significant enhancement of the well-established zenith scattered sunlight DOAS instruments, which are mainly sensitive to stratospheric absorbers [7]. MAX-DOAS systems have been further developed during the past few decades and are widely used for the retrieval of tropospheric trace gas concentrations with characteristic narrowband absorption structures in the ultraviolet (UV) and visible ranges [8–12]. MAX-DOAS is based on the analysis of scattered radiation spectra measured at multiple elevation viewing directions using the differential optical absorption spectroscopy (DOAS) technique [13]. MAX-DOAS measurements are highly sensitive to various absorbers, such as NO_2, HCHO, H_2O, BrO, CHOCHO and SO_2 in the lowest few kilometers of the atmosphere. Information about the vertical distribution of a trace gas can be obtained from a single elevation scan by applying proper inverse modeling approaches that combine the measurements with Radiative Transfer Model (RTM) simulations (e.g., [14–17]). The capability of retrieving trace gas vertical profiles, vertical column densities and surface concentrations with a generally high accuracy and temporal resolution makes the MAX-DOAS systems essential for air quality monitoring, supplementing point measurements of in situ instruments and satellite observations. Ground-based MAX-DOAS systems have been used in numerous recent publications for the assessment of air pollution, especially in urban environments, and for understanding of the physical and chemical processes in the boundary layer (e.g., [18,19]). Additionally, data derived from MAX-DOAS instruments are widely used for comparison and validation of multiple satellite products, including tropospheric NO_2 (e.g., [20–22]).

Even though ground-based MAX-DOAS is a well-established remote sensing technique for the determination of trace gas concentration levels in the troposphere and the application of such instruments to air quality monitoring is widespread, the sparsity of such systems on a global scale inhibits large-scale monitoring of NO_2. Satellite instruments do not suffer from this limitation; they provide daily global coverage and, thus, their importance to air quality, climate change and understanding of the dynamics in the boundary layer is widely recognized. Satellite observations contribute to the continuous monitoring of NO_2 on both regional and global scales, estimation of NO_x emission sources and provide valuable information for the understanding of NO_2 transport phenomena. Over the past decades, NO_2 has been continuously monitored from space by multiple satellite instruments, such as the Global Ozone Monitoring Experiment (GOME) on ERS-2 [23], Scanning Imaging Absorption SpectroMeter for Atmospheric CHartographY (SCIAMACHY) on ENVISAT [24], Ozone Monitoring Instrument (OMI) on EOS-Aura [25], Global Ozone Monitoring Experiment-2 (GOME-2) on MetOp A, B and C platforms [26] and, most recently, since October 2017 from the TROPOspheric Monitoring Instrument (TROPOMI) on board Sentinel-5 Precursor (S5P) [27]. The S5P/TROPOMI NO_2 observations have already demonstrated their monitoring capabilities in various air quality-related fields, such as estimating NO_x emissions at the urban scale [28,29] and evaluating the effect of the recent COVID-19 pandemic on NO_2 levels [30,31], while an extensive validation against global

ground-based measurements has been presented in [22]. The main disadvantages of such satellite instruments are their low temporal sampling with one or two overpasses per day at any given location, which does not allow the observation of diurnal cycles, as well as their coarse spatial resolution. With respect to the spatial sampling, the pixel size of the space borne instruments has been greatly improved, initially starting from several hundreds of kilometers (40×320 km^2 for GOME) to a few kilometers (13×24 km^2 for OMI) and currently to 3.5×5.5 km^2 for TROPOMI. This improvement, joined by the continuous efforts in improving the NO_2 data quality by updating the retrieval algorithms of S5P/TROPOMI, highly increases the usability of this dataset in numerous different scientific and research fields.

The main aims of this study are to assess the ability of the MAX-DOAS measurements to monitor the air quality in Thessaloniki in terms of tropospheric NO_2 by comparison with in situ data, and to validate the corresponding S5P/TROPOMI product, accounting also for the spatial features detected by the MAX-DOAS. By establishing the linkages among the three different sources of information on NO_2 in the area, we will set the scene for a future synergistic use of these datasets to achieve a more comprehensive characterization of NO_2 in Thessaloniki.

This article is structured as follows: In Section 2, a description is given for the instruments and data that are used in this study. In Section 3, the results of the NO_2 spatio-temporal variability using MAX-DOAS observations are presented along with comparisons with in situ measurements. In Section 4, the comparison and validation of S5P/TROPOMI observations using ground-based MAX-DOAS data from Thessaloniki are discussed, and in Section 5 the main conclusions of this study are summarized.

2. Data and Methodology

2.1. MAX-DOAS Observations

Monitoring of trace gases in the troposphere is routinely performed at the Laboratory of Atmospheric Physics (40.634° N, 22.956° E, 60 m above sea level), in the Aristotle University of Thessaloniki (LAP.AUTH), Greece, by multiple MAX-DOAS instruments. These systems have participated in various intercomparison and validation campaigns, such as the Cabauw Intercomparison of Nitrogen Dioxide Measuring Instruments 2 (CINDI-2, http://www.tropomi.eu/data-products/cindi-2/, accessed on 20 January 2023) and the TROpomi vaLIdation eXperiment 2019 (TROLIX'19, https://ruisdael-observatory.nl/trolix19-tropomi-validation-experiment-2019/, accessed on 20 January 2023), and they contribute data to global projects and networks, e.g., the Fiducial Reference Measurements for Ground-Based DOAS Air-Quality Observations (FRM4DOAS, https://frm4doas.aeronomie.be/, accessed on 20 January 2023), the Quality Assurance for Essential Climate Variables (QA4ECV, http://www.qa4ecv.eu/, accessed on 20 January 2023) and the Network for Detection of Atmospheric Composition Change (NDACC, https://ndacc.larc.nasa.gov/, accessed on 20 January 2023). The measurement site is located in an urban, moderately polluted environment, at the center of the city of Thessaloniki. The MAX-DOAS instruments have been gradually upgraded over the past decade by making changes to their design, using newer and improved spectrographs and by updating the operating software. Additionally, the processing and calibration of the recorded spectra have been further developed in order to increase their accuracy, improve their stability over time and provide data of higher quality.

In this study, the spatio-temporal variability of NO_2 over Thessaloniki is assessed by analyzing spectra recorded by a 2D MAX-DOAS system, Phaethon, which operates at LAP.AUTH since June 2020, using the DOAS technique. The entrance optics of the instrument are mounted on a two-axis tracker that allows for a full azimuthal and elevation rotation (0–360°). The system is configured to perform elevation scans, from the zenith to near the horizon, at different azimuth directions in the southern sector, as illustrated in Figure 1, since the other azimuths are partly or fully blocked by buildings of the city and the university campus. The elevation scans consist of measurements of scattered radiation

spectra at the elevation angles of 30, 15, 12, 10, 8, 6, 5, 4, 3, 2 and 1°, with about 1 min integration time per angle, in addition to a zenith-sky measurement (90°) prior to each scan that is used as a reference Fraunhofer spectrum (FRS) for the determination of the trace gas differential Slant Column Densities (dSCDs). The recorded spectra are analyzed using the QDOAS (version 3.2, September 2017) software that is developed by BIRA-IASB (https://uv-vis.aeronomie.be/software/QDOAS/, accessed on 20 January 2023). The NO_2 dSCDs are retrieved in the visible range, using the spectral fitting window 425–490 nm, following the recommendations from the CINDI-2 campaign [32]. Along with the NO_2 cross-sections at 298 K and 220 K [33], the following trace gas cross-sections are included in the DOAS analysis: O_3 at 223 K [34], O_4 at 293 K [35] and H_2O at 296 K [36]. A ring spectrum, calculated by QDOAS according to [37], was also included, and a fifth-order polynomial is used to remove the broadband spectral features. The MAX-DOAS system performs elevation scans at four different azimuth viewing directions, i.e., at 142° (SE), 185° (S), 220° (SW) and 255° (W) (Figure 1). The two former directions (SE and S) cross the city center and point to urban and suburban areas, while the other two directions (SW and W) cross a small portion of the city (about 1 km) and point towards the sea. The NO_2 vertical profile for each elevation scan is retrieved by applying the Mexican MAX-DOAS Fit (MMF) v2020_04 [38] inversion algorithm on the measured dSCDs, which is based on the Optimal Estimation Method (OEM). The NO_2 Vertical Column Densities (VCDs) are calculated by integrating the retrieved vertical profiles, while the "surface concentration" is the average concentration of the lowermost 200 m of the troposphere. MMF includes a quality flagging algorithm that is based on multiple criteria, and, in this study, the data that are flagged as erroneous were discarded from the analysis. In [39], more details are given about the instrumentation, the settings that are used for the retrieval of NO_2 dSCDs and the input parameters for the inversion algorithm that is applied for the retrieval of NO_2 vertical profiles.

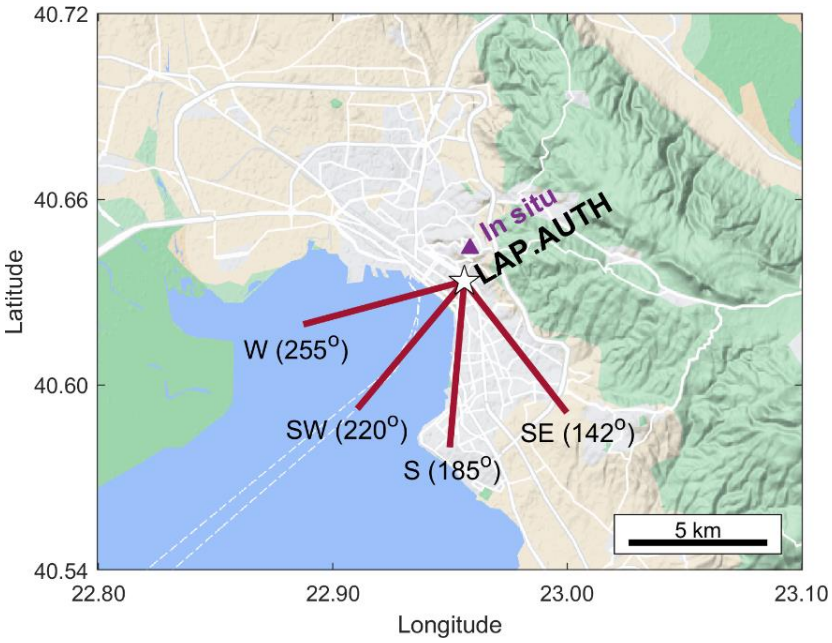

Figure 1. The locations of the MAX-DOAS instrument (white star) and the in situ NO_2 measurement site (purple triangle). The four different azimuth viewing directions of the MAX-DOAS observations are represented by the solid red lines. The base map is taken from © Google Maps, https://www.google.com/maps, accessed on 20 January 2023.

2.2. S5P/TROPOMI

The TROPOMI satellite instrument is a nadir-viewing imaging spectrometer that is mounted on the Sentinel-5 Precursor (S5P) platform. S5P was launched on 13 October

2017 and flies in a sun-synchronous orbit with a local overpass time at approximately 13:30 local time. TROPOMI covers a large wavelength range that extends from the UV to the shortwave infrared and provides daily global coverage. The main objective of the Copernicus Sentinel-5P mission is to perform atmospheric measurements with high spatial resolution around the globe. The initial, already high, spatial resolution of TROPOMI was 3.5×7 km^2 and from 6 August 2019 it was further improved to 3.5×5.5 km^2. The NO_2 data are continuously validated by the Mission Performance Center Validation Data Analysis Facility (MPC VDAF, http://mpc-vdaf.tropomi.eu/, accessed on 20 January 2023). In this study, we used the v2.2 S5P/TROPOMI NO_2 tropospheric vertical column density dataset that is publicly available via the ESA Sentinel-5P Product Algorithm Laboratory (S5P-PAL) containing modified Copernicus Sentinel data processed by S[&]T (https://data-portal.s5p-pal.com/products/no2.html, accessed on 20 January 2023). The overpass data for Thessaloniki cover the period from June 2020 to November 2022. Since clouds have a very strong impact on the column retrievals of all species (including NO_2), we filtered the TROPOMI data with a quality assurance value (qa_value) > 0.99, a criterion that filters out cloudy pixels for a cloud fraction > 20%. This strict filtering choice was made in order to ensure that all measurements under cloudy conditions were discarded from the analysis, even though the recommendation from the TROPOMI Algorithm Theoretical Basis Document (ATBD) of the tropospheric NO_2 data products (http://www.tropomi.eu/data-products/nitrogen-dioxide, accessed on 20 January 2023) is to filter the data with a qa_value > 0.75. We opted for the strict filtering since cloud presence is relatively less frequent in Thessaloniki and thus during the period of study the satellite sampling and the number of collocated TROPOMI and MAX-DOAS measurements was large enough to provide statistically robust comparison and validation results. The NO_2 concentration levels in Thessaloniki are mainly due to local NO_x emission sources, especially within the city center [40–43], where the MAX-DOAS system is installed. The relatively larger satellite footprint compared to the MAX-DOAS geometry would mainly result in a smoother perception of the NO_2 concentration. Hence, the TROPOMI tropospheric NO_2 column data are spatially averaged within 5 km from the overpass location.

2.3. In Situ Measurements

NO_2 concentrations near the surface are routinely monitored in Thessaloniki by in situ chemiluminescence analyzers that are administrated by the Network for Air Quality Monitoring of the Municipality of Thessaloniki (http://www.envdimosthes.gr, accessed on 20 January 2023). The main advantage of in situ instruments compared to remote sensing systems, such as the MAX-DOAS, is their relatively lower procurement cost and their ability to measure NO_2 concentrations continuously (also at nighttime) and irrespective of weather conditions, while the MAX-DOAS requires sunlight and thus its operation is limited to daytime. The highest temporal resolution of the in situ data that are publicly available is hourly averaged concentrations. The MAX-DOAS-derived diurnal and weekly cycles of the surface NO_2 concentrations are compared with in situ data measured in a background urban environment (40.644° N, 22.957° E, 174 m above sea level) (Figure 1). As described in [39], this particular site is selected because it is less affected by local NO_x traffic emissions and the reported data are considered more representative of the average NO_2 concentrations in the local boundary layer. The in situ dataset that is used in this study spans from 1 June 2020 to 30 November 2022 with very few gaps in the time series due to maintenance of the instrumentation.

3. Results and Discussion

In this study the MAX-DOAS tropospheric NO_2 vertical columns, referred to hereafter as NO_2 VCDs, are calculated by integrating the NO_2 vertical profiles, retrieved by the inversion algorithm (MMF) which is applied to the dSCDs. The NO_2 VCDs can also be derived by applying either the geometrical approximation [7] to the dSCDs measured at 30 or 15° elevation angles or to a mix of them, or by using proper differential Air Mass

Factors (dAMFs), calculated by RTM simulations (e.g., [20]). In any case, the NO_2 vertical columns are a good indicator of the pollution levels around a measurement site; however, when inversion techniques are applied, additional information can be retrieved for the concentration levels near the surface, which is essential especially in the context of air quality monitoring. In this section, the temporal and spatial variability of NO_2 VCDs and surface concentrations using MAX-DOAS observations is discussed. The temporal variability is assessed by calculating seasonal (Section 3.1), diurnal (Section 3.2) and weekly cycles (Section 3.3) for different seasons, which are compared with the in situ data. The spatial NO_2 variations are investigated (Section 3.4) by comparing the concentration levels at the four azimuth viewing directions for two different time periods during the day.

3.1. Seasonal Variability

Figure 2 shows the time series of the daily and monthly median NO_2 VCDs (upper panel) and the corresponding surface concentrations (bottom panel) retrieved by the MAX-DOAS for the period of study. The data are aggregated separately for the urban (SE and S) and rural (W and SW) azimuths (blue and green lines with markers, respectively). The gray dots represent the MAX-DOAS daily median values, while the red line with markers indicates the monthly median values, derived from the in situ instrument. The in situ NO_2 time series is plotted against the MAX-DOAS surface NO_2 concentrations only, in order to compare meaningful quantities. The error bars of the monthly median values indicate the monthly variability as the interquartile range (IQR), i.e., the difference between the 75th and 25th percentiles. In June 2020 and April 2022, the MAX-DOAS was configured to record spectra only in the SW direction and thus measurements pointing towards urban areas are not available during these months.

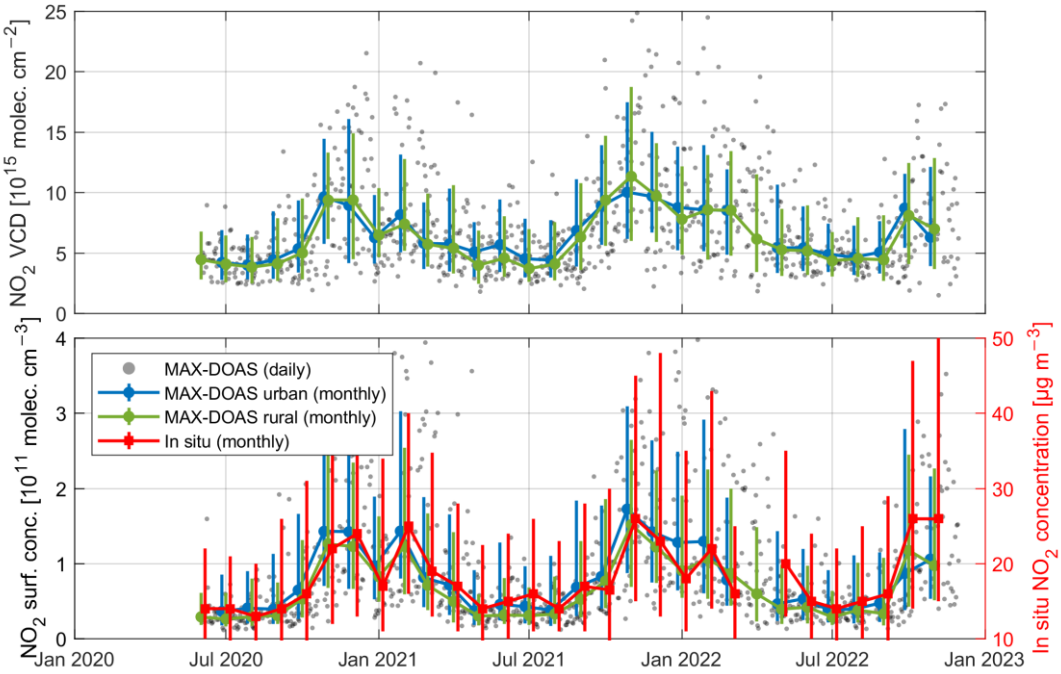

Figure 2. The time series of NO_2 vertical columns (**upper**) and surface concentrations (**bottom**) retrieved by the MAX-DOAS in Thessaloniki, Greece (gray dots represent the daily medians, while the blue and green lines with markers represent the monthly medians for the urban and rural azimuth viewing directions, respectively). The monthly median NO_2 surface concentrations measured by the in situ instrument are shown in red (right ordinate). The error bars of the monthly medians represent the variability as the interquartile range.

Here, and in the following sections, the MAX-DOAS and in situ surface concentrations are presented in different axes (due to their different units) to demonstrate the co-variability

of the two datasets since a quantitative comparison between the two systems is beyond the scope of this study. It also follows that since these two time series are not temporally synchronized, even though both medians represent the daylight measurements, the monthly median NO_2 concentrations have not necessarily been derived by measurements acquired at the same time intervals during each day. In this work, we mainly aim to conduct a qualitative comparison and investigate whether similar temporal NO_2 variation patterns are captured by the two instruments, indicating that they can equally contribute to air quality monitoring. In a previous study covering a shorter time period [39], a direct 1:1 comparison between MAX-DOAS and in situ NO_2 hourly mean concentrations showed that the MAX-DOAS was low-biased by ~55–60%. This was attributed to the fact that the MAX-DOAS probes air masses along the line of sight of a few kilometers, while the air quality station measurements are conducted in situ. A similar comparison of the daily and monthly mean surface concentrations for the whole time period can be found in Appendix A.

The NO_2 VCDs and surface concentrations show a similar seasonal cycle, i.e., lower values during summer and higher values during winter. Similar results using MAX-DOAS measurements in urban environments have been reported for other locations (e.g., [18,44–46]). In urban environments, NO_2 is mainly distributed in the lowermost troposphere, usually within the first kilometer, since its emission sources are mainly located close to the ground (e.g., road transport emissions). Thus, the NO_2 VCDs are mostly affected by the concentration levels in the lowermost layers of the troposphere and hence the vertical columns and surface concentrations are expected to reveal similar patterns. The seasonal NO_2 variability captured for the urban and rural azimuths is similar for the whole period, with average differences (rural–urban) of about −5% for the VCDs and −18% for the surface concentrations. However, shorter-term temporal variations are masked in monthly values, and as it will be discussed later in Section 3.4, differences between azimuths can be larger when shorter time intervals are considered. The seasonal cycles of the surface concentrations retrieved by the in situ and the MAX-DOAS measurements are in very good agreement. The lower NO_2 levels during all summer periods, the significant reduction in January 2021 and the peaks during the cold periods (e.g., November, December 2020; February, November 2021; and October, November 2022) are well captured by both instruments. The median NO_2 VCD for the period of study retrieved by the MAX-DOAS is $5.94 \pm 4.90 \times 10^{15}$ molecules/cm^2 and the median NO_2 surface concentration is $0.61 \pm 0.83 \times 10^{11}$ molecules/cm^3. The lowermost monthly median VCDs and surface concentrations were reported in July 2020 (4.16×10^{15} molecules/cm^2 and 0.31×10^{11} molecules/cm^3, respectively), while the highest were found in November 2021 (10.73×10^{15} molecules/cm^2 and 1.61×10^{11} molecules/cm^3, respectively). The monthly variability (i.e., the interquartile range), presented by the error bars, is significant, reaching maximum values in November 2021. The monthly variability captured by the in situ data is even larger, since the site is affected more by local emissions. The monthly median of the in situ data in May 2022 was unusually high, affected by days that were characterized by extreme NO_2 levels, probably due to very local events and activities that could not be captured by the MAX-DOAS. The relatively lower NO_2 concentrations that were reported by both systems during summer are related to the reduced emission sources (e.g., absence of domestic heating) and to the shorter lifetime of NO_2 caused by the enhanced photolysis rate due to stronger solar radiation.

3.2. Diurnal Cycles

In the boundary layer, NO_2 is a short-lived product, with typical lifetime of a few hours, depending on the season [47], and, as a result, the NO_2 amounts are expected to be highly variable during the day. The diurnal variability of the NO_2 surface concentrations retrieved by the MAX-DOAS and the in situ instrument for all seasons is presented in Figure 3, in order to evaluate the performance of the instruments under different pollution levels and to investigate their diurnal cycles in more detail. The seasonal hourly mean

NO_2 concentrations were calculated when at least 100 measurements were available. In this section (and also in Section 3.3), all azimuth viewing directions of the MAX-DOAS (Figure 1) were included in the calculation of the means.

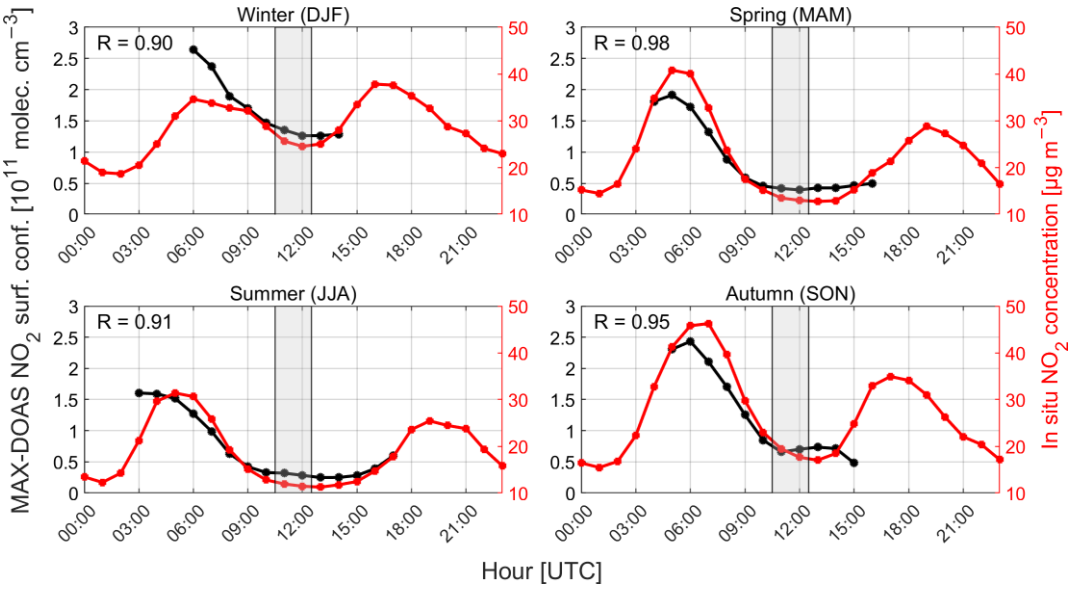

Figure 3. The diurnal variability of NO_2 surface concentrations revealed by the MAX-DOAS (black) and the in situ (red) measurements for all seasons. The gray-shaded rectangles indicate the range of S5P/TROPOMI overpass times for Thessaloniki.

The in situ instrument reports NO_2 concentrations throughout the day (and also during the night), while the MAX-DOAS can only operate when solar scattered radiation is present. Thus, the secondary NO_2 peak that is evident in the in situ data at ~16:00–17:00 UTC during autumn and winter and at ~19:00–20:00 UTC during spring and summer cannot be revealed by the MAX-DOAS. However, both instruments show very similar diurnal cycles for all seasons. The Pearson's correlation coefficients (R) for the two datasets are displayed in the plots and they range from 0.90 during winter to 0.98 during spring, indicating that the two systems can equally contribute to air quality monitoring.

The early morning NO_2 peak (~1.9–2.6 $\times$ 10^{11} molecules/cm^3 in winter, spring and autumn) in the MAX-DOAS data that is found during the rush hours (i.e., between ~04:00 and 06:00 UTC) is due to the increased morning traffic emissions and to the accumulated NO_2 in the boundary layer during the night. This morning peak is reduced by 25–30% during summer (reaching ~1.61 $\times$ 10^{11} molecules/cm^3). Afterwards, the NO_2 concentrations rapidly drop as a result of enhanced consumption processes (photochemical destruction). The reduction is stronger and faster in summer and spring due to increased solar radiation. The NO_2 surface concentrations reach minimum values for all seasons between ~11:00 and 13:00 UTC (approximately 0.25 and 1.25 $\times$ 10^{11} molecules/cm^3 in summer and winter, respectively), when the sun is high, leading to an increased photolysis rate in addition to the reduced traffic-related emissions. In the afternoon and evening, the photolysis rate weakens and NO_2 begins to accumulate, leading to the secondary peak as mentioned already. This afternoon increase is only marginally captured by the MAX-DOAS during winter and summer due to the lack of sunlight and, hence, observations. The high NO_2 concentrations that were reported in the morning by both instruments and at night by the in situ instrument only are also attributed to the shallow boundary layer due to the absence of solar radiation and the lower air temperatures. Especially during winter, when the boundary layer height in Thessaloniki reaches minimum values [48], the vertical displacement of ~100 m of the two sites is no longer negligible. In this case, even though a very good correlation is found (R = 0.9), the MAX-DOAS reports higher morning surface

NO_2 concentrations than in the other seasons, with a higher reduction rate between 06:00 to 09:00 UTC compared to the in situ instrument.

3.3. Day of the Week Variability

NO_2 is emitted in the troposphere by anthropogenic activities (e.g., industrial and road transport emission sources) that usually follow a weekly cycle. Normally, such activities are enhanced during the working days, and they are significantly reduced at weekends, leading to strong weekday-to-weekend variations of NO_2 concentrations in urban environments, a phenomenon that is known as the "weekend effect". The weekend effect has been investigated in the past using both ground-based MAX-DOAS data (e.g., [18,19,42,49,50]) and satellite observations (e.g., [51–53]). In these studies, a significant reduction of the NO_2 concentration in weekends is reported, with a clear Sunday minimum of up to 50% compared to the working days. Here, we investigate the day of week variability of NO_2 surface concentrations in Thessaloniki using MAX-DOAS observations and in situ measurements for comparison. Figure 4 shows the average weekly cycles of NO_2 surface concentrations for all seasons measured by both instruments.

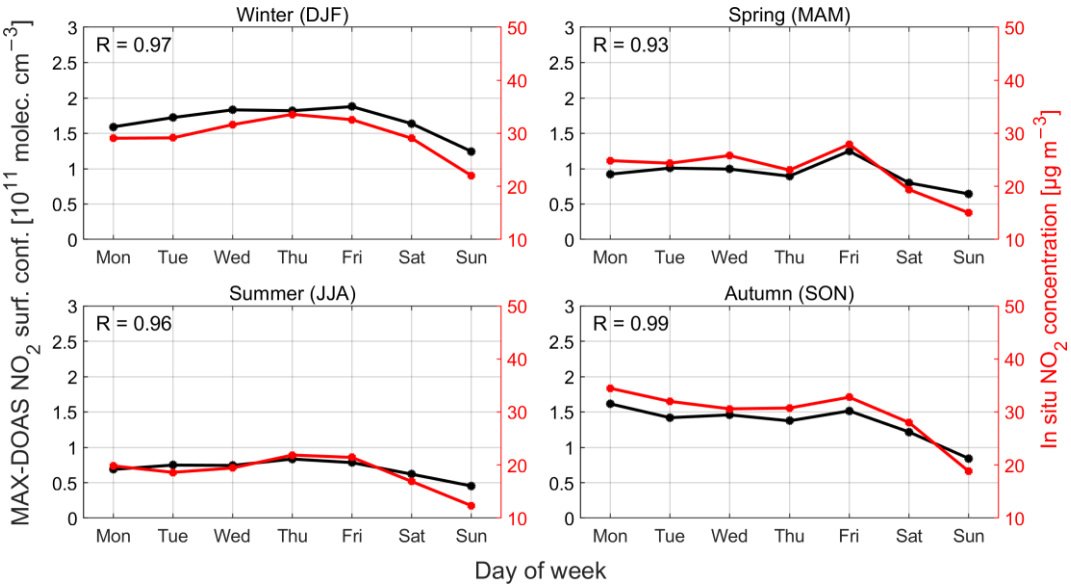

Figure 4. The day of week variability of NO_2 surface concentrations revealed by the MAX-DOAS (black) and the in situ (red) measurements for all seasons.

The two datasets reveal similar weekly patterns with Pearson's correlation coefficients that range between 0.93 (in spring) and 0.99 (in autumn). The weekend effect for all seasons is investigated by comparing the mean NO_2 surface concentrations on the weekends (Saturday and Sunday) and the traditional resting day of Sunday alone with the mean concentration during the working days (Monday to Friday). Significantly lower NO_2 concentrations are found for both datasets during weekends for all seasons, i.e., the MAX-DOAS (in situ) reports a reduction of 19% (18%) in winter, 29% (31%) in spring, 30% (28%) in summer and 30% (27%) in autumn. The reduction rate is even larger on Sundays, i.e., 30% (29%) in winter, 37% (40%) in spring, 40% (39%) in summer and 43% (41%) in autumn. The two systems reveal that the weekend effect is more evident during the warm period and less distinct in winter. The stronger reduction in the warm period is associated with the shorter atmospheric lifetime of NO_2, due to higher photochemical destruction rates, resulting in less accumulation in the working days. Additionally, the expansion of the boundary layer to higher altitudes in summer due to stronger solar radiation allows for a greater dispersion of NO_2, leading to lower concentrations at the lowermost layers compared with the cold period. A reduction of the NO_2 vertical column with increasing

boundary layer height in Thessaloniki, especially during summer, was also found by [43] using MAX-DOAS measurements and chemical transport model simulations.

Figure 5 shows the diurnal variation of tropospheric NO_2 VCDs (top row) and surface concentrations (bottom row) in a weekly cycle retrieved by the MAX-DOAS over Thessaloniki for each day of the week. The analysis was conducted separately for the cold period (October–February, left column) and the warm period (May–September, right column). The variability of the NO_2 levels in Thessaloniki from Monday to Friday is not very pronounced; however, the weekend effect is strong for both time periods.

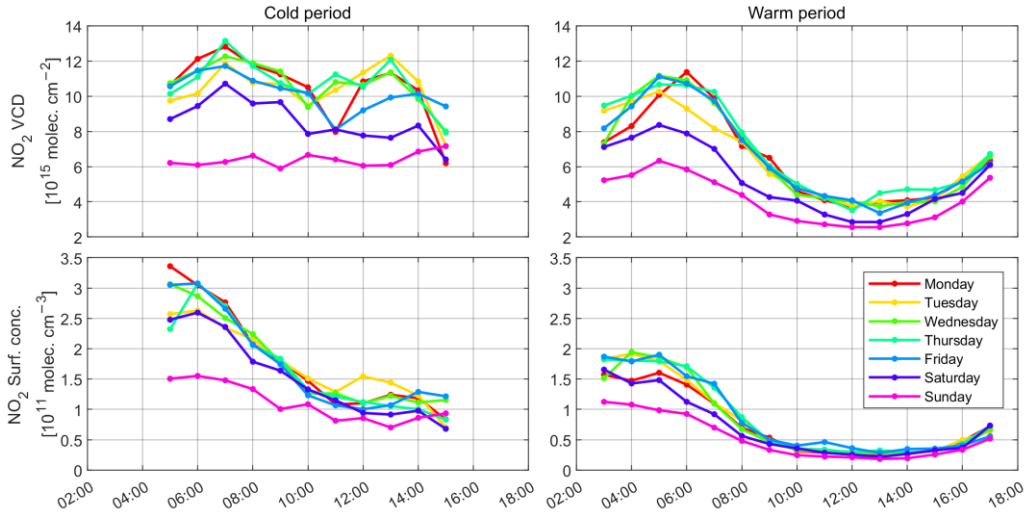

Figure 5. The mean diurnal variability of NO_2 vertical columns and surface concentrations derived by the MAX-DOAS observations for each day of the week for the cold and warm periods.

On Saturdays (dark blue line in Figure 5), the NO_2 amounts are generally lower than on the working days but are of comparable magnitude in the early morning and late afternoon. The strongest reduction of the NO_2 vertical column and surface concentrations is found on Sundays (purple line in Figure 5) throughout the day. This is mainly related to the decreased human activities on the resting day and especially to the absence of NO_x emissions from heavy road transport to and from work. As already discussed in Section 3.2, the diurnal variability patterns of tropospheric NO_2 are rather different for the two time periods, mainly due to different NO_x emission strengths and the lifetime of NO_2 in the troposphere, in addition to the different boundary layer structure that has a strong effect on the accumulation and dispersion of NO_2.

3.4. Spatial Distribution

Since in urban environments, especially in large cities, emission sources of various sizes and strengths are distributed in different areas, the NO_2 concentrations can vary rapidly in space. In situ (point measurements) or MAX-DOAS observations at one azimuth (1D systems), that provide information about the NO_2 content in a particular direction, are usually not representative for the NO_2 amounts in the surrounding areas. However, by using MAX-DOAS measurements at multiple azimuths (2D systems), valuable information for the assessment of the NO_2 spatial distribution can be retrieved, allowing for the investigation of possible NO_2 horizontal inhomogeneities and a better characterization of the NO_2 field around the measurement site. In this study, the spatial variability of NO_2 over Thessaloniki was investigated by comparing the NO_2 vertical columns and surface concentrations measured at different azimuth viewing directions (see Figure 1) over the period of study. These viewing geometries can be roughly distinguished to those representing urban/suburban environments, across the city center and pointing to heavy-traffic roads (azimuths of 142° and 185°) and to those pointing towards the sea (220° and 255°). On short timescales (e.g., on a daily basis), spatial differences in the NO_2 amounts can

occur. Figure 6 shows an example of the diurnal variability of the NO_2 VCDs during a sunny summer day for all azimuth directions, which are represented by lines of different colors. On this day, 15% of the data were flagged as invalid by the inversion algorithm (MMF) and thus they were rejected from the analysis, leading to some missing values in the time series. The morning peak and the secondary afternoon increase of NO_2 that were related to enhanced traffic emissions, along with the strong reduction of NO_2 at noon due to increased photochemical reactions (see also Section 3.2), are well captured in all viewing directions. However, the NO_2 columns in the SE direction were systematically and significantly larger compared to the other azimuths, especially in the morning, likely related to the inhomogeneous emissions within the city.

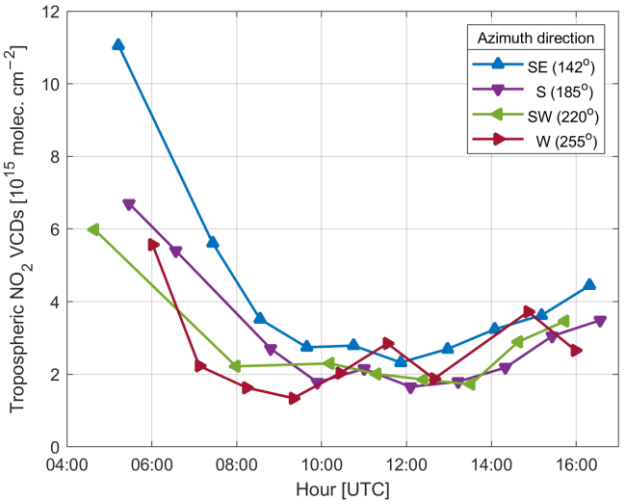

Figure 6. An example of the NO_2 VCDs diurnal variability for all azimuth viewing directions of the MAX-DOAS during a clear-sky summer day (30 July 2022).

As already discussed in Section 3.2, the concentration of NO_2 in the boundary layer changes rapidly with time (both in the short- and long-term), prohibiting a detailed investigation of its horizontal distribution. Even on a daily basis, a full measurement sequence for all viewing directions lasts for about 1 hour (~15 min per elevation scan for each azimuth and ~2 min per scan for dark signal measurements). This constrains the time step of measurements at each azimuth angle to at most one per hour. The NO_2 variability over the whole period of study (~2.5 years) was analyzed separately for the cold and warm periods, aiming at the investigation of possible differences in spatial distribution patterns. In order to reduce the effect of the NO_2 temporal variability, the analysis was focused on two periods of different, but less variable, NO_2 levels, i.e., in the morning, when NO_2 is high, and during noon hours, when the NO_2 concentrations reach minimum values. Anthropogenic activities that lead to the emission of tropospheric NO_2 peak at different times during the cold and warm periods (Figure 5). Hence, in our analysis, morning hours were considered as between 06:00 and 09:00 UTC for the cold period and between 04:00 and 07:00 UTC for the warm period. Similarly, the time intervals 10:00–12:00 and 11:00–14:00 UTC were used for the noon hours for the cold and warm periods, respectively.

Figure 7 shows the normalized median NO_2 VCDs and surface concentrations for the four azimuths (*x* axis, see also Figure 1). The data were normalized by dividing the medians with the average VCD or surface concentration of all azimuths for the corresponding period, while the error bars indicate the variability for each azimuth as the interquartile range. The top row of panels represents the NO_2 VCDs and the bottom row the NO_2 surface concentrations, while each column refers to a different time period of the day. In the morning, the normalized NO_2 VCDs and surface concentrations along the different azimuths reveal a generally homogenous spatial distribution for the cold period (Figure 7, blue dots). This is probably related to the relatively longer lifetime of NO_2 in the troposphere, due to weaker

photochemical destruction, that allows stronger dispersion of the pollutant, leading to better horizontal mixing. Furthermore, meteorological parameters, (e.g., wind direction and speed) can also affect the horizontal dispersion of NO_2. Although a detailed investigation of these effects is beyond the scope of this study, the influence of wind speed and direction is briefly addressed in Appendix B. During the warm period (Figure 7, red squares), the NO_2 VCDs also show a similar (homogenous) horizontal distribution. However, despite the large variability, the NO_2 surface concentrations for the SE direction are generally higher than in the other azimuths, while the lowest concentrations are reported for the SW direction. The SW direction points towards the sea (Figure 1) and the effective horizontal path extends over the bay, where NO_2 is expected to be significantly lower than in the urban environment. Even though the W direction is also towards the sea, it crosses part of the western sector of the urban Thessaloniki, where industrial activities take place, and thus the reported NO_2 concentrations are generally higher than in the SW direction. Finally, the SE direction crosses the entire city center and an urban area of persistent traffic-related NO_x emissions, resulting in locally increased NO_2 loads.

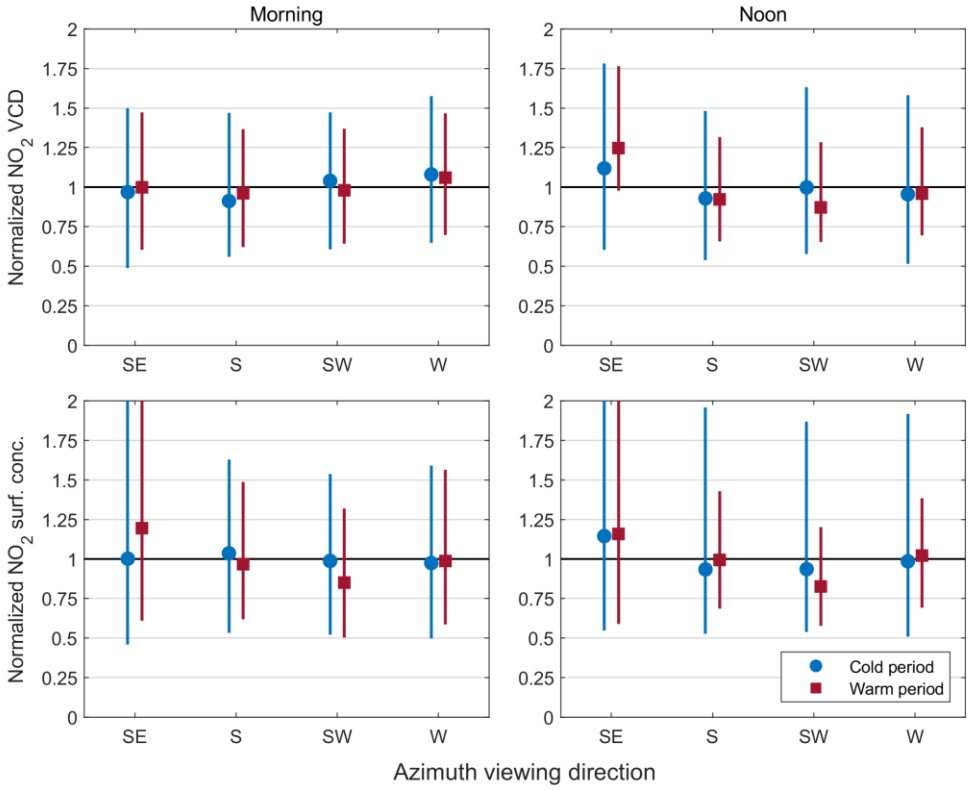

Figure 7. Distribution of the normalized MAX-DOAS measurements of NO_2 VCDs (**top row**) and surface concentrations (**bottom row**) for all azimuth viewing angles during morning (**left column**) and noon (**right column**) hours. Data are presented separately for the cold (blue) and warm (red) periods.

During noon hours, when the NO_2 levels overall significantly drop, the median NO_2 VCDs and surface concentrations are higher for the SE direction in both periods. This effect is stronger during the warm period due to the enhanced NO_2 photolysis rates and the generally weaker winds that suppress the dispersion, leading to less homogenous horizontal distribution. Similar results have been reported in [46]. For the same reasons that are discussed for the morning hours, the median NO_2 concentrations for the SW direction are significantly lower than the other viewing directions, especially during the warm period.

The variability of NO_2 in all azimuths is large, due to highly variable emission sources, and thus quantitative estimates cannot be easily unveiled from Figure 7. Hence, the percentage differences of the median NO_2 VCDs and surface concentrations for each azimuth from the average of all directions are summarized in Table 1 for the cold and warm periods. In the morning, the median NO_2 surface concentrations are ~20% above average for the SE direction and ~15% below average for the SW direction during the warm period. For noon hours, the median NO_2 VCDs are ~12% (25%) higher for the cold (warm) period, while the respective surface concentrations are ~15% (16%) higher. Similarly, the noon NO_2 load in the SW direction is approximately 17% lower than in the other azimuths.

Table 1. Percentage difference of the median NO_2 VCDs and surface concentrations for each azimuth from the average concentration of all azimuths for the morning and noon hours and for the cold and warm periods. The highest differences are marked in bold.

		SE (142°)	**S (185°)**	**SW (220°)**	**W (255°)**
		cold/warm	cold/warm	cold/warm	cold/warm
Morning	NO_2 vertical columns	−3.2/−0.1%	−8.8/−3.9%	4.0/−2.0%	8.0/6.0%
	NO_2 surface concentrations	0.2/**19.4%**	3.6/−3.3%	−1.2/**−14.9%**	−2.6/−1.27%
Noon	NO_2 vertical columns	**11.9/24.7%**	−7.1/−7.7%	−0.2/−12.9%	−4.5/−4.1%
	NO_2 surface concentrations	**14.5/15.8%**	−6.6/−0.6%	−6.4/**−17.4%**	−1.5/2.1%

The statistical significance of the differences between the NO_2 VCDs and surface concentrations for the rural (SW) and urban (SE) azimuths was assessed by the Student's t-test. Despite the large range of variability, the differences were found to be statistically significant at the 95% confidence level in all cases, except for the VCDs in the morning, due to the more homogenous horizontal distribution of NO_2, as previously discussed. Statistically significant differences were found also between other azimuths, but the most consistent pattern is that for the SE direction.

4. Comparison with S5P/TROPOMI

In this section, the tropospheric NO_2 vertical columns retrieved by TROPOMI for Thessaloniki (considering only cloud-free satellite pixels) are compared and validated using collocated ground-based MAX-DOAS measurements.

Since TROPOMI data are limited to only one overpass per day, short-term (e.g., diurnal) NO_2 variations cannot be investigated with satellite data. TROPOMI passes over Thessaloniki between approximately 10:30 and 12:30 UTC (Figure 3), when the NO_2 concentrations are usually low for the reasons discussed in Section 3.2. However, NO_2 is a highly variable pollutant and, thus, in order to compare meaningful results, the collocated ground-based and satellite observations should have a short time difference. In this study, the collocations are calculated by averaging MAX-DOAS measurements within ±15 min of the satellite overpass time. Figure 8 shows the time series of the collocated tropospheric NO_2 vertical column measurements in box-and-whisker plots over the whole period of study (30 months), from June 2020 to November 2022. The seasonal variations of NO_2 are well captured by both instruments and the reported seasonal patterns are similar over the period of study. The higher tropospheric NO_2 columns during winter are consistent with the results presented in Section 3.1. Furthermore, higher variability of NO_2 VCDs is found during the cold period for both ground-based and satellite observations, especially for those of the MAX-DOAS. This is expected since NO_x emissions are stronger during wintertime, which, combined with the lower photolysis rate of NO_2 due to limited sunlight and the more variable weather patterns, results in higher spatio-temporal variability. The highest monthly variations, represented by the interquartile range, are found during December 2020, February 2021 and December 2021 (ranging between 5.72–13.17 × 10^{15} molecules/cm^2 for the MAX-DOAS and 4.90–6.59 × 10^{15} molecules/cm^2

for TROPOMI). These are consistent with Figure 2, indicating that pollution events were well captured by both ground-based and satellite instruments.

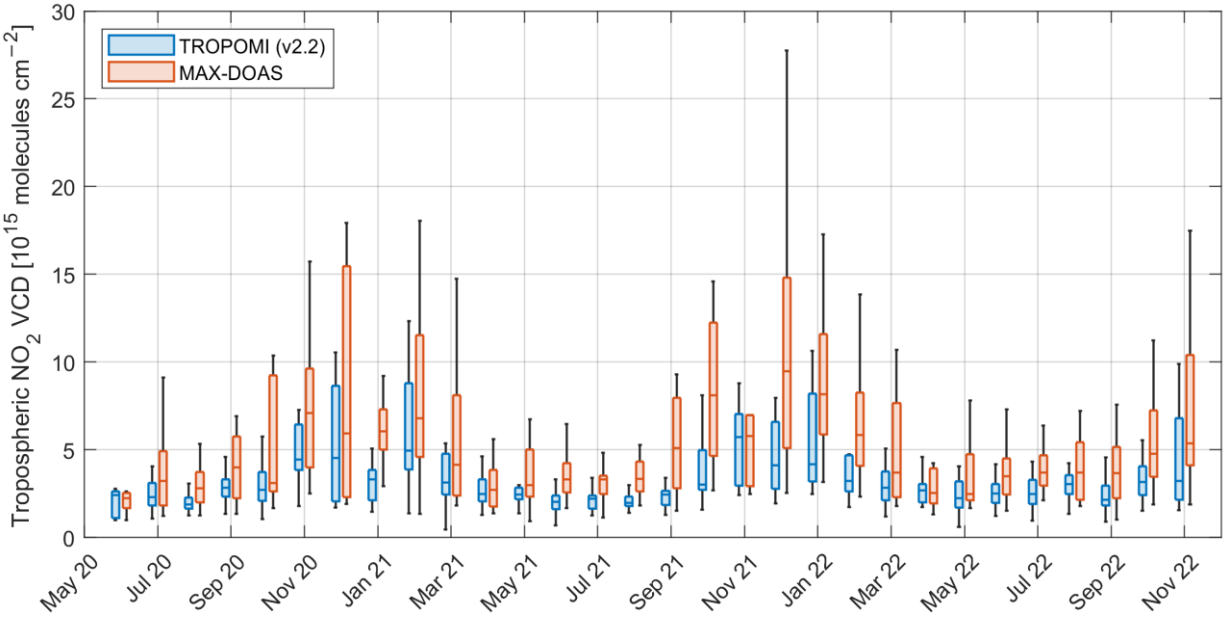

Figure 8. Time series of monthly mean tropospheric NO_2 vertical columns in Thessaloniki from collocated ground-based MAX-DOAS and S5P/TROPOMI observations for the period June 2020–November 2022.

Figure 9 presents the comparison of TROPOMI tropospheric NO_2 vertical columns against MAX-DOAS measurements in scatter plots for the four seasons of the whole period of study. Overall, TROPOMI systematically reports lower NO_2 columns than the MAX-DOAS. The underestimation of satellite-derived tropospheric NO_2 compared to MAX-DOAS observations is also found in recent publications (e.g., [54–56]) and it is more evident in highly polluted and in extremely highly polluted environments [22].

The MAX-DOAS probes air masses along the line of sight of the telescope, pointing at different elevation angles, from near the horizon to the zenith. The measurements are sensitive to local emissions located on this line of sight and at distances up to a few kilometers. The NO_2 columns that are reported by satellite instruments are essentially averaged over the sub-satellite pixel area (3.5×5.5 km^2 for S5P/TROPOMI), which contains different emissions sources, resulting, generally, in the underestimation of the NO_2 columns. The highest correlation between the two instruments is found in winter (R = 0.75), while significantly lower correlations are found during spring (R = 0.6), autumn (R = 0.6) and summer (R = 0.44). For all seasons, a negative bias is found for TROPOMI with median differences of $-2.91 \pm 3.77 \times 10^{15}$ molecules/cm^2 in winter, $-0.57 \pm 2.13 \times 10^{15}$ molecules/cm^2 in spring, $-1.04 \pm 1.55 \times 10^{15}$ molecules/cm^2 in summer and $-1.42 \pm 2.97 \times 10^{15}$ molecules/cm^2 in autumn. These biases correspond to mean fractional biases of about -55% during winter, -21% in spring and -40% in summer and autumn.

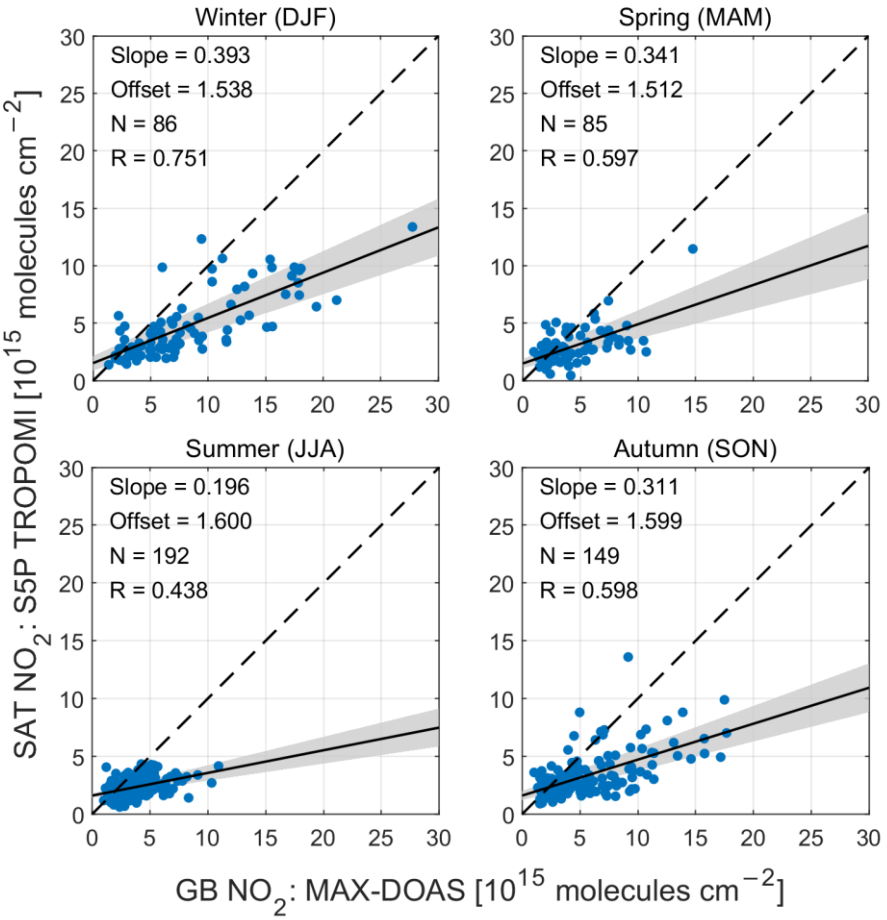

Figure 9. Scatter plots of the daily collocated tropospheric NO_2 VCDs that are reported by the MAX-DOAS and S5P/TROPOMI for all seasons. The gray shaded areas represent the 95% confidence interval of the linear regression fit (solid black line).

Figure 10 shows the consolidated comparison (i.e., without seasonal discrimination) of TROPOMI and MAX-DOAS tropospheric NO_2 columns in a scatter plot (Figure 10a) over the whole period of study. The blue markers indicate the daily collocated observations, while the red dots represent the monthly mean vertical columns. Figure 10b shows the frequency distribution of the absolute daily differences between TROPOMI and MAX-DOAS. The black and red dashed lines indicate the median and mean difference, respectively, while the solid magenta lines represent the 25th and 75th percentiles of the distribution. The correlation coefficient of the daily collocated data is 0.72, with slope and offset values of 0.37 and 1.24, respectively. For the monthly means, the statistics are significantly improved with R = 0.89 and slope and offset values of 0.49 and 0.71, respectively. A clear negative bias is found with median and mean differences of -1.19 and -1.93 ($\times 10^{15}$ molecules/cm^2), respectively (which corresponds to a mean fractional bias of approximately -37%), and an interquartile range of 2.89×10^{15} molecules/cm^2. These results are consistent with the findings in the latest issue of the quarterly Routine Operations Consolidated Validation Report (http://mpc-vdaf.tropomi.eu/, accessed on 20 January 2023), where for the S5P/TROPOMI tropospheric NO_2 product, a median bias of -1.8×10^{15} molecules/cm^2 (about -35%) was found over the full satellite mission using NDACC-affiliated MAX-DOAS data from 30 measurement sites.

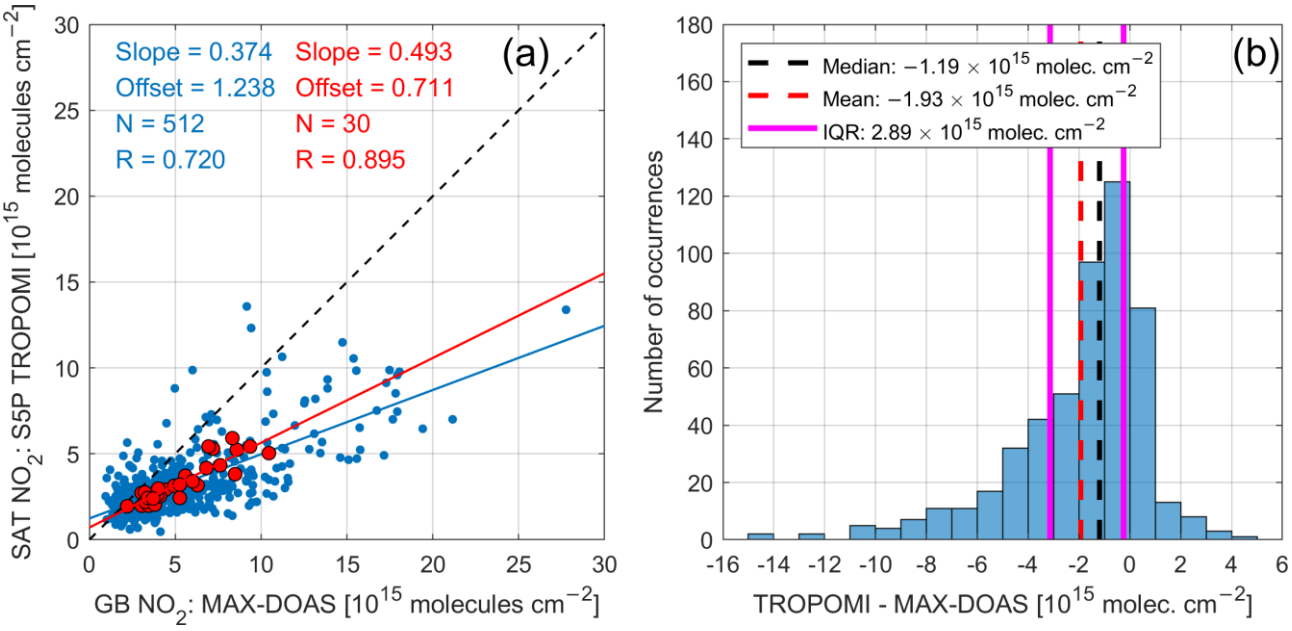

Figure 10. The consolidated comparison of tropospheric NO_2 vertical columns (**a**) between the MAX-DOAS and S5P/TROPOMI for the daily (blue) and monthly mean (red) collocated measurements and the frequency distribution (**b**) of their absolute differences.

5. Summary and Conclusions

In this study, the spatio-temporal variability of tropospheric NO_2 over Thessaloniki, Greece, was investigated using vertical column and surface concentration data that were retrieved by MAX-DOAS observations during the period June 2020–November 2022. The NO_2 seasonal, diurnal and weekly cycles were investigated and the surface concentrations that were retrieved by the MAX-DOAS were compared with in situ data from a nearby air quality station, which is mostly unaffected by local emissions and, hence, is more representative of the average NO_2 levels in the local boundary layer. The comparison of the two ground-based datasets was conducted in order to evaluate the performance of the MAX-DOAS instrument in the context of air quality monitoring in Thessaloniki.

The tropospheric NO_2 VCDs and surface concentrations, retrieved by the MAX-DOAS, show a similar seasonal cycle, i.e., lower values during summer and higher values during winter. The higher columns in winter are due to enhanced anthropogenic emissions (e.g., domestic heating) and the longer lifetime of NO_2 in this season. Hourly mean NO_2 surface concentrations measured by the MAX-DOAS reveal a clear diurnal pattern with an early morning peak during the rush hours, followed by a reduction around noon as a result of stronger photolysis rates. The increased morning concentrations are due to the enhanced traffic-related NO_x emissions and the accumulation of NO_2 in the boundary layer during the night. The morning peak during summer is significantly reduced (by approximately 25–30%) compared with the other seasons. Additionally, the NO_2 day of the week variability and the weekend effect were investigated. The NO_2 surface concentrations retrieved by the MAX-DOAS were significantly lower on the weekend (by 20–30%), especially on Sundays (by 30–40%), compared with the working days. In all cases, the NO_2 temporal variations that were captured by the MAX-DOAS are in agreement with the in situ measurements with Pearson's correlation coefficients ranging from 0.90 to 0.99, indicating that the two systems are equally capable of monitoring the variability of NO_2 over Thessaloniki.

The NO_2 spatial variability was investigated by comparing the concentrations reported by the MAX-DOAS for four azimuth viewing directions. In order to reduce the effect of the NO_2 temporal variability, the analysis was conducted separately for the morning hours, when the NO_2 levels are high, and for noon hours, when the NO_2 concentrations reach minimum values. On a long timescale (i.e., during the 30 months in this study), the spatial

NO_2 variability is masked by the strong short-term temporal variations. However, despite the large variability, higher NO_2 concentrations of up to 25% were found for the SE azimuth that crosses the entire city center and extends over an urban area compared with azimuths towards the sea (e.g., SW). Differences between the SE and SW directions were statistically significant at the 95% confidence level for all cases, except for the VCDs in the morning.

The tropospheric NO_2 VCDs in Thessaloniki, retrieved by the MAX-DOAS, were compared with collocated measurements of the TROPOMI instrument on board the Sentinel-5P satellite, aiming at the validation of the satellite product against the well-established ground-based observations. The comparisons were conducted for all seasons in order to investigate any seasonal effects and to evaluate their agreement under both low and high NO_2 concentration levels. The seasonal NO_2 variations were well captured by both instruments, with increased VCDs during the cold period due to enhanced emissions and a reduction during the warm period as a result of stronger photochemical destruction of NO_2. Even though a generally good correlation was found between MAX-DOAS and TROPOMI ($R = 0.72$ and $R = 0.89$ for the daily and monthly means, respectively), TROPOMI underestimates the tropospheric NO_2 VCDs by approximately 55% in winter, 21% in spring and 40% during autumn and summer. The consolidated median and mean absolute differences (i.e., without seasonal discrimination) are -1.19 and -1.93 ($\times 10^{15}$ molecules/cm^2), respectively, and they correspond to a mean fractional bias of approximately -37%, which is in agreement with the latest S5P MPC VDAF validation report (http://mpc-vdaf.tropomi.eu/, accessed on 20 January 2023). This clearly negative bias is mainly caused by the much larger satellite footprint, resulting in a smoother perception of the NO_2 concentrations, while the MAX-DOAS measurements are affected more by local emissions.

Author Contributions: Conceptualization, A.B. and D.K.; Investigation, D.K.; Methodology, D.K., M.-E.K., A.B. and D.B.; Resources, D.K., M.-E.K. and P.T.; Software, D.K. and M.-E.K.; Formal analysis, D.K. and M.-E.K.; Data curation, D.K., M.-E.K. and P.T.; Validation, D.K. and M.-E.K.; Supervision, A.B. and D.B.; Writing—original draft, D.K.; Writing—review and editing, D.K., M.-E.K., A.B., D.B. and P.T. All authors have read and agreed to the published version of the manuscript.

Funding: This research is co-financed by Greece and the European Union (European Social Fund-ESF) through the Operational Programme «Human Resources Development, Education and Lifelong Learning» in the context of the project "Strengthening Human Resources Research Potential via Doctorate Research—2nd Cycle" (MIS-5000432), implemented by the State Scholarships Foundation (ΙΚΥ).

Institutional Review Board Statement: Not applicable.

Informed Consent Statement: Not applicable.

Data Availability Statement: The MAX-DOAS data used in this study are available from the corresponding author upon request. The air quality monitoring station data are available from the Municipality of Thessaloniki, Department of Environment, upon request. The meteorological data are publicly available from https://meteo3.geo.auth.gr/stations/orofi_Data.HTML, accessed on 20 January 2023. The S5P/TROPOMI data are publicly available from the Sentinel-5P Product Algorithm Laboratory (S5P-PAL; S5P-PAL Data portal) and contain modified Copernicus Sentinel data processed by S[&]T.

Acknowledgments: We acknowledge support of this work by the project "PANhellenic infrastructure for Atmospheric Composition and climatE change" (MIS 5021516), which is implemented under the Action "Reinforcement of the Research and Innovation Infrastructure", funded by the Operational Programme "Competitiveness, Entrepreneurship and Innovation" (NSRF 2014–2020) and co-financed by Greece and the European Union (European Regional Development Fund). Results presented in this work have been produced using the Aristotle University of Thessaloniki (AUTh) High Performance Computing Infrastructure and Resources. M.-E.K. would like to acknowledge the support provided by the AUTh IT Center throughout the progress of this research work. We thank Caroline Fayt (caroline.fayt@aeronomie.be), Michel Van Roozendael (michelv@aeronomie.be) and Thomas Danckaert (thomas.danckaert@aeronomie.be) for the free use of the QDOAS software, Robert Spurr

for the free use of the VLIDORT radiative transfer code package and Martina Michaela Friedrich (martina.m.friedrich@aeronomie.be) for providing the MMF algorithm.

Conflicts of Interest: The authors declare no conflict of interest.

Appendix A

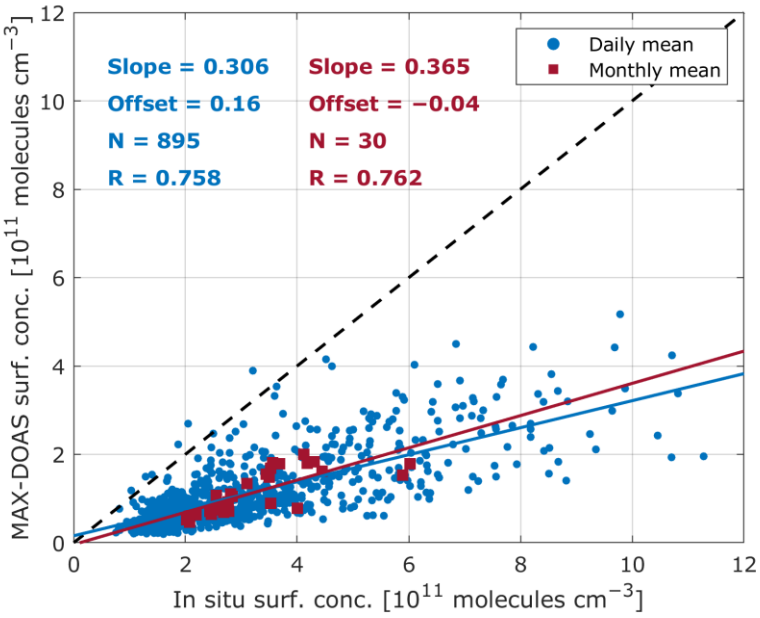

Figure A1. Scatter plot of the daily and monthly mean surface concentrations that were retrieved by the MAX-DOAS and the in situ instruments for the period of study.

Appendix B. Prevailing Meteorological Conditions over Thessaloniki

This section describes briefly the dominant wind patterns over Thessaloniki for the period of study (June 2020 to November 2022). Wind speed and direction (averaged over 10 min intervals) are continuously monitored by a meteorological station that is installed on the rooftop (~25 m above ground) of the Department of Meteorology and Climatology building, which is located inside the University campus at a horizontal distance of about 300 m from the location of the MAX-DOAS instrument. The wind data are publicly available via the corresponding website (https://meteo3.geo.auth.gr/stations/orofi_Data.HTML, accessed on 20 January 2023).

Figure A2 shows the wind rose diagrams over Thessaloniki for summer and winter. In summer, the prevailing wind directions are S–SW and are usually characterized by low wind speeds (on average < 3 m/s), while northern winds are less frequent. The presence of southern winds is a result of the coastal orientation of the city (Figure 1) and the temperature difference between the land and the sea (which is more pronounced during the warm period due stronger solar radiation) that allow the formation of sea breeze circulation [57–59]. The wind pattern is different in winter with the dominant winds blowing from N–NW directions being generally stronger (reaching speeds of over 8 m/s) than in summer. According to [57], the wind patterns in the cold period are caused by the combination of low-pressure systems over the Mediterranean Sea and anticyclones over central Europe.

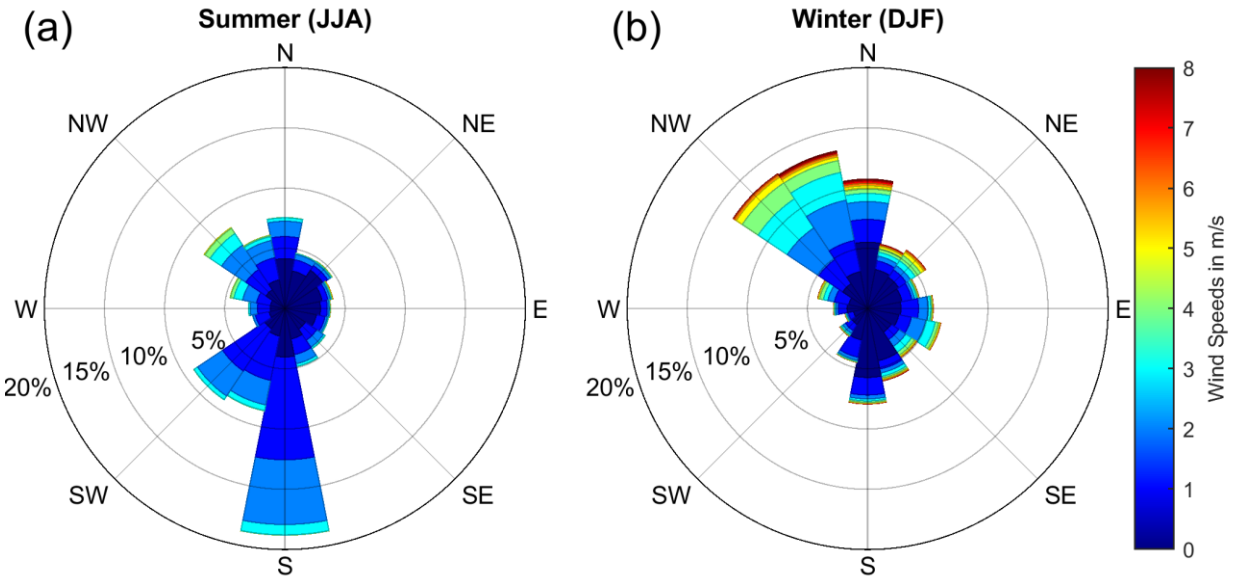

Figure A2. Wind rose diagrams (binned by 22.5°) over Thessaloniki during summer (**a**) and winter (**b**) for the period June 2020 to November 2022.

The variability of the NO_2 concentration levels is not only related to the spatial distribution of its emission sources, but it is also associated with certain meteorological parameters, such as wind direction and speed, since the latter significantly contribute to the vertical and horizontal dispersion of air pollutants. The effect of wind speed on the tropospheric vertical columns and surface concentrations of NO_2 in Thessaloniki for the two dominant wind directions, N–NW and S–SW, is depicted in Figure A3. For northern wind regimes, the NO_2 VCDs and surface concentrations have similar variation patterns, i.e., higher NO_2 amounts are reported for low wind speeds, followed by a clear gradual reduction with increasing wind speed. This is expected, since such wind conditions contribute more efficiently to the dispersion of NO_2, which is transported from the urban area towards the sea. For southern winds, a reduction in the NO_2 levels is also evident for low to moderate wind speeds (up to 4 m/s); however, a non-negligible enhancement is found for higher wind speeds (>4 m/s), especially for the surface concentrations. This finding is consistent with similar results in [58] and [40]. According to these studies, given the topography of the greater area of Thessaloniki, such conditions favor the accumulation of air pollutants. Furthermore, these wind-direction-related patterns of NO_2 could also be associated with larger-scale NO_2 transport events from southern Greece; however, additional investigation is required for the determination of NO_2 emission sources and the assessment of NO_2 transport phenomena, which is beyond the scope of this study.

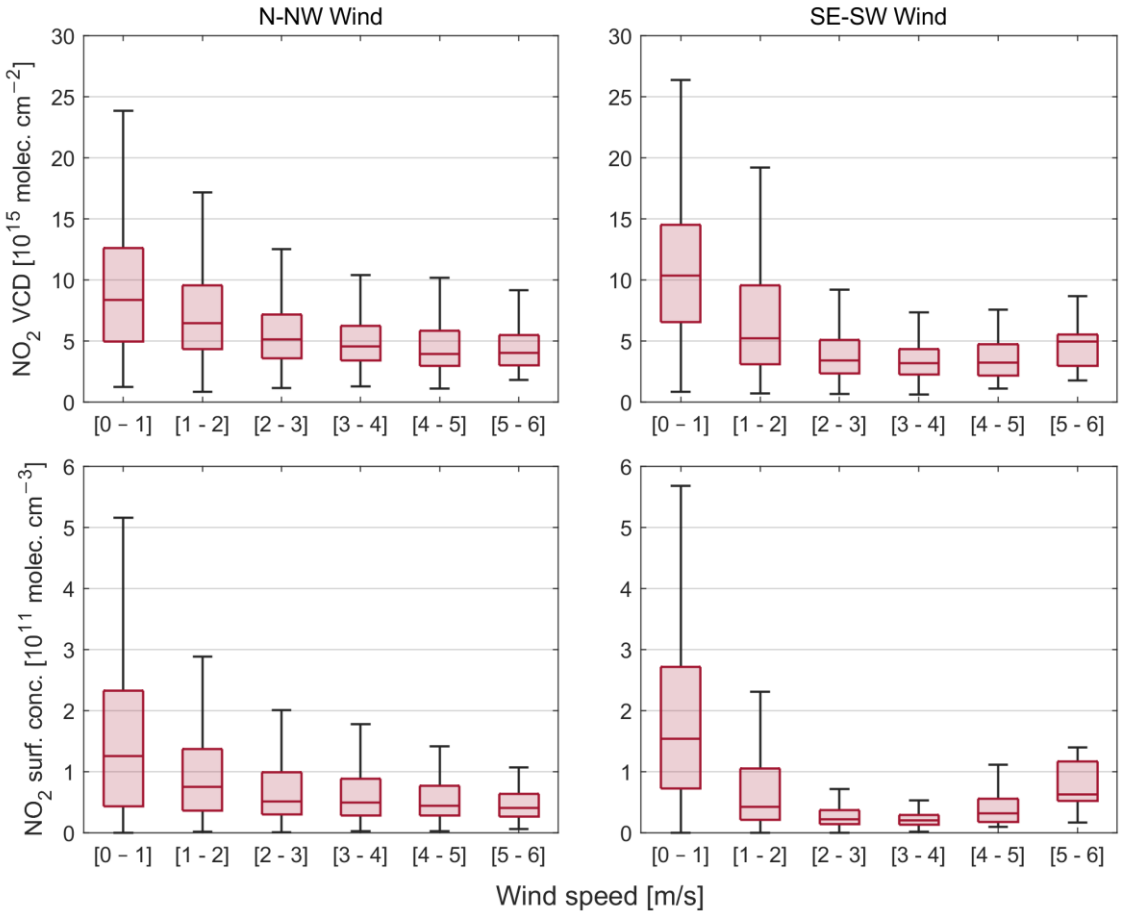

Figure A3. Tropospheric vertical columns (**upper** panels) and surface concentrations (**bottom** panels) of NO_2 as a function of wind speed. The left and right columns correspond to N–NW and S–SW wind directions, respectively.

References

1. World Health Organization (WHO). *Ambient Air Pollution: A Global Assessment of Exposure and Burden of Disease*; World Health Organisation: Bonn, Germany, 2016; ISBN 9789241511353.
2. Seinfeld, J.H.; Pandis, S.N.; Noone, K. Atmospheric Chemistry and Physics: From Air Pollution to Climate Change. *Phys. Today* **1998**, *51*, 88–90. [CrossRef]
3. Solomon, S.; Portmann, R.W.; Sanders, R.W.; Daniel, J.S.; Madsen, W.; Bartram, B.; Dutton, E.G. On the role of nitrogen dioxide in the absorption of solar radiation. *J. Geophys. Res. Atmos.* **1999**, *104*, 12047–12058. [CrossRef]
4. Lee, D.; Köhler, I.; Grobler, E.; Rohrer, F.; Sausen, R.; Gallardo-Klenner, L.; Olivier, J.; Dentener, F.; Bouwman, A. Esti-mations of global no, emissions and their uncertainties. *Atmos. Environ.* **1997**, *31*, 1735–1749. [CrossRef]
5. Zhang, R.; Tie, X.; Bond, D.W. Impacts of anthropogenic and natural NOx sources over the U.S. on tropospheric chemistry. *Proc. Natl. Acad. Sci. USA* **2003**, *100*, 1505–1509. [CrossRef] [PubMed]
6. European Environmental Agency, EEA. *Air Quality in Europe—2020 Report*; Publications Office of the European Union: Luxembourg, 2020; ISBN 978-92-9480-292-7. ISSN 1977-8449. Available online: https://www.eea.europa.eu/publications/air-quality-in-europe-2020-report (accessed on 20 January 2023).
7. Hönninger, G.; von Friedeburg, C.; Platt, U. Multi axis differential optical absorption spectroscopy (MAX-DOAS). *Atmos. Chem. Phys.* **2004**, *4*, 231–254. [CrossRef]
8. Hönninger, G.; Platt, U. Observations of BrO and its vertical distribution during surface ozone depletion at Alert. *Atmos. Environ.* **2002**, *36*, 2481–2489. [CrossRef]
9. Bobrowski, N.; Hönninger, G.; Galle, B.; Platt, U. Detection of bromine monoxide in a volcanic plume. *Nature* **2003**, *423*, 273–276. [CrossRef]
10. Wittrock, F.; Oetjen, H.; Richter, A.; Fietkau, S.; Medeke, T.; Rozanov, A.; Burrows, J.P. MAX-DOAS measurements of atmospheric trace gases in Ny-Ålesund—Radiative transfer studies and their application. *Atmos. Chem. Phys.* **2004**, *4*, 955–966. [CrossRef]
11. Wagner, T.; Dix, B.; Friedeburg, C.V.; Frieß, U.; Sanghavi, S.; Sinreich, R.; Platt, U. MAX-DOAS O_4measurements: A new technique to derive information on atmospheric aerosols-Principles and information content. *J. Geophys. Res. Atmos.* **2004**, *109*. [CrossRef]

12. Van Roozendael, M.; Fayt, C.; Post, P.; Hermans, C.; Lambert, J. *Retrieval of Tropospheric BrO and NO_2 from UV-Visible Observations*; Springer: Berlin/Heidelberg, Germany, 2004; pp. 155–165. [CrossRef]
13. Platt, U.; Stutz, J. *Differential Optical Absorption Spectroscopy: Principles and Applications, Physics of Earth and Space Environments*; Springer: Berlin/Heidelberg, Germany, 2008.
14. Irie, H.; Takashima, H.; Kanaya, Y.; Boersma, K.F.; Gast, L.; Wittrock, F.; Brunner, D.; Zhou, Y.; Van Roozendael, M. Eight-component retrievals from ground-based MAX-DOAS observations. *Atmos. Meas. Tech.* **2011**, *4*, 1027–1044. [CrossRef]
15. Vlemmix, T.; Hendrick, F.; Pinardi, G.; De Smedt, I.; Fayt, C.; Hermans, C.; Piters, A.; Wang, P.; Levelt, P.; Van Roozendael, M. MAX-DOAS observations of aerosols, formaldehyde and nitrogen dioxide in the Beijing area: Comparison of two profile retrieval approaches. *Atmos. Meas. Tech.* **2015**, *8*, 941–963. [CrossRef]
16. Bösch, T.; Rozanov, V.; Richter, A.; Peters, E.; Rozanov, A.; Wittrock, F.; Merlaud, A.; Lampel, J.; Schmitt, S.; de Haij, M.; et al. BOREAS—A new MAX-DOAS profile retrieval algorithm for aerosols and trace gases. *Atmos. Meas. Tech.* **2018**, *11*, 6833–6859. [CrossRef]
17. Beirle, S.; Dörner, S.; Donner, S.; Remmers, J.; Wang, Y.; Wagner, T. The Mainz profile algorithm (MAPA). *Atmos. Meas. Tech.* **2019**, *12*, 1785–1806. [CrossRef]
18. Ma, J.Z.; Beirle, S.; Jin, J.L.; Shaiganfar, R.; Yan, P.; Wagner, T. Tropospheric NO_2 vertical column densities over Beijing: Results of the first three years of ground-based MAX-DOAS measurements (2008–2011) and satellite validation. *Atmos. Meas. Tech.* **2013**, *13*, 1547–1567. [CrossRef]
19. Wang, Y.; Lampel, J.; Xie, P.; Beirle, S.; Li, A.; Wu, D.; Wagner, T. Ground-based MAX-DOAS observations of tropospheric aerosols, NO_2, SO_2 and HCHO in Wuxi, China, from 2011 to 2014. *Atmos. Chem. Phys.* **2017**, *17*, 2189–2215. [CrossRef]
20. Drosoglou, T.; Bais, A.F.; Zyrichidou, I.; Kouremeti, N.; Poupkou, A.; Liora, N.; Giannaros, C.; Koukouli, M.E.; Balis, D.; Melas, D. Comparisons of ground-based tropospheric NO_2 MAX-DOAS measurements to satellite observations with the aid of an air quality model over the Thessaloniki area, Greece. *Atmos. Meas. Tech.* **2017**, *17*, 5829–5849. [CrossRef]
21. Pinardi, G.; Van Roozendael, M.; Hendrick, F.; Theys, N.; Abuhassan, N.; Bais, A.; Boersma, F.; Cede, A.; Chong, J.; Donner, S.; et al. Validation of tropospheric NO_2 column meas-urements of GOME-2A and OMI using MAX-DOAS and direct sun network observations. *Atmos. Meas. Tech.* **2020**, *13*, 6141–6174. [CrossRef]
22. Verhoelst, T.; Compernolle, S.; Pinardi, G.; Lambert, J.-C.; Eskes, H.J.; Eichmann, K.-U.; Fjæraa, A.M.; Granville, J.; Niemeijer, S.; Cede, A.; et al. Ground-based validation of the Copernicus Sentinel-5P TROPOMI NO_2 measurements with the NDACC ZSL-DOAS, MAX-DOAS and Pandonia global networks. *Atmos. Meas. Tech.* **2021**, *14*, 481–510. [CrossRef]
23. Burrows, J.P.; Weber, M.; Buchwitz, M.; Rozanov, V.; Ladstätter-Weißenmayer, A.; Richter, A.; DeBeek, R.; Hoogen, R.; Bramstedt, K.; Eichmann, K.-U.; et al. The Global Ozone Monitoring Experiment (GOME): Mission Concept and First Scientific Results. *J. Atmos. Sci.* **1999**, *56*, 151–175. [CrossRef]
24. Bovensmann, H.; Burrows, J.P.; Buchwitz, M.; Frerick, J.; Noël, S.; Rozanov, V.V.; Chance, K.V.; Goede, A.P.H. SCI-AMACHY: Mission Objectives and Measurement Modes. *J. Atmos. Sci.* **1999**, *56*, 127–150. [CrossRef]
25. Levelt, P.; van den Oord, G.; Dobber, M.; Malkki, A.; Visser, H.; de Vries, J.; Stammes, P.; Lundell, J.; Saari, H. The ozone monitoring instrument. *IEEE Trans. Geosci. Remote Sens.* **2006**, *44*, 1093–1101. [CrossRef]
26. Munro, R.; Lang, R.; Klaes, D.; Poli, G.; Retscher, C.; Lindstrot, R.; Huckle, R.; Lacan, A.; Grzegorski, M.; Holdak, A.; et al. The GOME-2 instrument on the Metop series of satellites: Instrument design, calibration, and level 1 data processing—An overview. *Atmos. Meas. Tech.* **2016**, *9*, 1279–1301. [CrossRef]
27. Veefkind, J.; Aben, I.; McMullan, K.; Förster, H.; de Vries, J.; Otter, G.; Claas, J.; Eskes, H.; de Haan, J.; Kleipool, Q.; et al. TROPOMI on the ESA Sentinel-5 Precursor: A GMES mission for global observations of the atmospheric composition for climate, air quality and ozone layer applications. *Remote Sens. Environ.* **2012**, *120*, 70–83. [CrossRef]
28. Goldberg, D.L.; Lu, Z.; Streets, D.G.; de Foy, B.; Griffin, D.; McLinden, C.A.; Lamsal, L.N.; Krotkov, N.A.; Eskes, H. Enhanced Capabilities of TROPOMI NO_2: Estimating NOX from North American Cities and Power Plants. *Environ. Sci. Technol.* **2019**, *53*, 12594–12601. [CrossRef]
29. Lorente, A.; Boersma, K.F.; Eskes, H.J.; Veefkind, J.P.; van Geffen, J.H.G.M.; de Zeeuw, M.B.; Denier van der Gon, H.A.C.; Beirle, S.; Krol, M.C. Quantification of nitrogen oxides emissions from build-up of pollution over Paris with TROPOMI. *Sci. Rep.* **2019**, *9*, 20033. [CrossRef]
30. Bauwens, M.; Compernolle, S.; Stavrakou, T.; Müller, J.-F.; Van Gent, J.; Eskes, H.; Levelt, P.F.; Van Der, A.R.; Veefkind, J.P.; Vlietinck, J.; et al. Impact of Coronavirus Outbreak on NO_2 Pollution Assessed Using TROPOMI and OMI Observations. *Geophys. Res. Lett.* **2020**, *47*, e2020GL087978. [CrossRef] [PubMed]
31. Levelt, P.F.; Zweers, D.C.S.; Aben, I.; Bauwens, M.; Borsdorff, T.; De Smedt, I.; Eskes, H.J.; Lerot, C.; Loyola, D.G.; Romahn, F.; et al. Air quality impacts of COVID-19 lockdown measures detected from space using high spatial resolution observations of multiple trace gases from Sentinel-5P/TROPOMI. *Atmos. Meas. Tech.* **2022**, *22*, 10319–10351. [CrossRef]
32. Kreher, K.; Van Roozendael, M.; Hendrick, F.; Apituley, A.; Dimitropoulou, E.; Frieß, U.; Richter, A.; Wagner, T.; Lampel, J.; Abuhassan, N.; et al. Intercomparison of NO_2, O_4, O_3 and HCHO slant column measurements by MAX-DOAS and zenith-sky UV–visible spec-trometers during CINDI-2. *Atmos. Meas. Tech.* **2020**, *13*, 2169–2208. [CrossRef]
33. Vandaele, A.; Hermans, C.; Simon, P.; Carleer, M.; Colin, R.; Fally, S.; Mérienne, M.; Jenouvrier, A.; Coquart, B. Meas-urements of the NO_2 absorption cross-section from 42 000 cm^{-1} to 10 000 cm^{-1} (238–1000 nm) at 220 K and 294 K. *J. Quant. Spectrosc. Ra.* **1998**, *59*, 171–184. [CrossRef]

34. Serdyuchenko, A.; Gorshelev, V.; Weber, M.; Chehade, W.; Burrows, J.P. High spectral resolution ozone absorption cross-sections—Part 2: Temperature dependence. *Atmos. Meas. Tech.* **2014**, *7*, 625–636. [CrossRef]
35. Thalman, R.; Volkamer, R. Temperature dependent absorption cross-sections of O_2–O_2 collision pairs between 340 and 630 nm and at atmospherically relevant pressure. *Phys. Chem. Chem. Phys.* **2013**, *15*, 15371–15381. [CrossRef] [PubMed]
36. Rothman, L.S.; Gordon, I.E.; Barber, R.J.; Dothe, H.; Gamache, R.R.; Goldman, A.; Perevalov, V.; Tashkun, S.A.; Tennyson, J. HITEMP, the high-temperature molecular spectroscopic database. *J. Quant. Spectrosc. Radiat. Transf.* **2010**, *111*, 2139–2150. [CrossRef]
37. Chance, K.V.; Spurr, R.J.D. Ring effect studies: Rayleigh scattering, including molecular parameters for rotational Raman scattering, and the Fraunhofer spectrum. *Appl. Opt.* **1997**, *36*, 5224–5230. [CrossRef]
38. Friedrich, M.M.; Rivera, C.; Stremme, W.; Ojeda, Z.; Arellano, J.; Bezanilla, A.; García-Reynoso, J.A.; Grutter, M. NO_2 vertical profiles and column densities from MAX-DOAS measurements in Mexico City. *Atmos. Meas. Tech.* **2019**, *12*, 2545–2565. [CrossRef]
39. Karagkiozidis, D.; Friedrich, M.M.; Beirle, S.; Bais, A.; Hendrick, F.; Voudouri, K.A.; Fountoulakis, I.; Karanikolas, A.; Tzoumaka, P.; Van Roozendael, M.; et al. Retrieval of tropospheric aerosol, NO_2, and HCHO vertical profiles from MAX-DOAS observations over Thessaloniki, Greece: Intercomparison and validation of two inversion algo-rithms. *Atmos. Meas. Tech.* **2022**, *15*, 1269–1301. [CrossRef]
40. Poupkou, A.; Nastos, P.; Melas, D.; Zerefos, C. Climatology of Discomfort Index and Air Quality Index in a Large Urban Mediterranean Agglomeration. *Water Air Soil Pollut.* **2011**, *222*, 163–183. [CrossRef]
41. Koukouli, M.-E.; Skoulidou, I.; Karavias, A.; Parcharidis, I.; Balis, D.; Manders, A.; Segers, A.; Eskes, H.; van Geffen, J. Sudden changes in nitrogen dioxide emissions over Greece due to lockdown after the outbreak of COVID-19. *Atmos. Meas. Tech.* **2021**, *21*, 1759–1774. [CrossRef]
42. Koukouli, M.-E.; Pseftogkas, A.; Karagkiozidis, D.; Skoulidou, I.; Drosoglou, T.; Balis, D.; Bais, A.; Melas, D.; Hatzianastassiou, N. Air Quality in Two Northern Greek Cities Revealed by Their Tropospheric NO_2 Levels. *Atmosphere* **2022**, *13*, 840. [CrossRef]
43. Skoulidou, I.; Koukouli, M.-E.; Manders, A.; Segers, A.; Karagkiozidis, D.; Gratsea, M.; Balis, D.; Bais, A.; Gerasopoulos, E.; Stavrakou, T.; et al. Evaluation of the LOTOS-EUROS NO_2 simulations using ground-based measurements and S5P/TROPOMI observations over Greece. *Atmos. Meas. Tech.* **2021**, *21*, 5269–5288. [CrossRef]
44. Hendrick, F.; Müller, J.-F.; Clémer, K.; Wang, P.; De Mazière, M.; Fayt, C.; Gielen, C.; Hermans, C.; Ma, J.Z.; Pinardi, G.; et al. Four years of ground-based MAX-DOAS observations of HONO and NO_2 in the Beijing area. *Atmos. Chem. Phys.* **2014**, *14*, 765–781. [CrossRef]
45. Blechschmidt, A.-M.; Arteta, J.; Coman, A.; Curier, L.; Eskes, H.; Foret, G.; Gielen, C.; Hendrick, F.; Marécal, V.; Meleux, F.; et al. Comparison of tropospheric NO_2 columns from MAX-DOAS re-trievals and regional air quality model simulations. *Atmos. Chem. Phys.* **2020**, *20*, 2795–2823. [CrossRef]
46. Chan, K.L.; Wiegner, M.; van Geffen, J.; De Smedt, I.; Alberti, C.; Cheng, Z.; Ye, S.; Wenig, M. MAX-DOAS measurements of tropospheric NO_2 and HCHO in Munich and the comparison to OMI and TROPOMI satellite observations. *Atmos. Meas. Tech.* **2020**, *13*, 4499–4520. [CrossRef]
47. Beirle, S.; Boersma, K.F.; Platt, U.; Lawrence, M.G.; Wagner, T. Megacity Emissions and Lifetimes of Nitrogen Oxides Probed from Space. *Science* **2011**, *333*, 1737–1739. [CrossRef] [PubMed]
48. Siomos, N.; Balis, D.S.; Voudouri, K.A.; Giannakaki, E.; Filioglou, M.; Amiridis, V.; Papayannis, A.; Fragkos, K. Are EARLINET and AERONET climatologies consistent? The case of Thessaloniki, Greece. *Atmos. Meas. Tech.* **2018**, *18*, 11885–11903. [CrossRef]
49. Gratsea, M.; Vrekoussis, M.; Richter, A.; Wittrock, F.; Schönhardt, A.; Burrows, J.; Kazadzis, S.; Mihalopoulos, N.; Gerasopoulos, E. Slant column MAX-DOAS measurements of nitrogen dioxide, formaldehyde, glyoxal and oxygen dimer in the urban environment of Athens. *Atmos. Environ.* **2016**, *135*, 118–131. [CrossRef]
50. Schreier, S.F.; Richter, A.; Peters, E.; Ostendorf, M.; Schmalwieser, A.W.; Weihs, P.; Burrows, J.P. Dual ground-based MAX-DOAS observations in Vienna, Austria: Evaluation of horizontal and temporal NO_2, HCHO, and CHOCHO distributions and comparison with independent data sets. *Atmos. Environ. X* **2019**, *5*, 100059. [CrossRef]
51. Beirle, S.; Platt, U.; Wenig, M.; Wagner, T. Weekly cycle of NO_2 by GOME measurements: A signature of anthropogenic sources. *Atmos. Chem. Phys.* **2003**, *3*, 2225–2232. [CrossRef]
52. Stavrakou, T.; Müller, J.-F.; Bauwens, M.; Boersma, K.F.; van Geffen, J. Satellite evidence for changes in the NO_2 weekly cycle over large cities. *Sci. Rep.* **2020**, *10*, 10066. [CrossRef]
53. Goldberg, D.L.; Anenberg, S.C.; Kerr, G.H.; Mohegh, A.; Lu, Z.; Streets, D.G. TROPOMI NO_2 in the United States: A Detailed Look at the Annual Averages, Weekly Cycles, Effects of Temperature, and Correlation with Surface NO_2 Concen-trations. *Earth's Future* **2021**, *9*, e2020EF001665. [CrossRef]
54. Griffin, D.; Zhao, X.; McLinden, C.A.; Boersma, F.; Bourassa, A.; Dammers, E.; Degenstein, D.; Eskes, H.; Fehr, L.; Fioletov, V.; et al. High-Resolution Mapping of Nitrogen Dioxide With TROPOMI: First Results and Validation Over the Canadian Oil Sands. *Geophys. Res. Lett.* **2019**, *46*, 1049–1060. [CrossRef]
55. Dimitropoulou, E.; Hendrick, F.; Pinardi, G.; Friedrich, M.M.; Merlaud, A.; Tack, F.; De Longueville, H.; Fayt, C.; Hermans, C.; Laffineur, Q.; et al. Validation of TROPOMI tropospheric NO_2 columns using dual-scan mul-ti-axis differential optical absorption spectroscopy (MAX-DOAS) measurements in Uccle, Brussels. *Atmos. Meas. Tech.* **2020**, *13*, 5165–5191. [CrossRef]

56. Zhao, X.; Griffin, D.; Fioletov, V.; McLinden, C.; Cede, A.; Tiefengraber, M.; Müller, M.; Bognar, K.; Strong, K.; Boersma, F.; et al. Assessment of the quality of TROPOMI high-spatial-resolution NO_2 data products in the Greater Toronto Area. *Atmos. Meas. Tech.* **2020**, *13*, 2131–2159. [CrossRef]
57. Moussiopoulos, N.; Vlachokostas, C.; Tsilingiridis, G.; Douros, I.; Hourdakis, E.; Naneris, C.; Sidiropoulos, C. Air quality status in Greater Thessaloniki Area and the emission reductions needed for attaining the EU air quality legislation. *Sci. Total Environ.* **2009**, *407*, 1268–1285. [CrossRef]
58. Kassomenos, P.; Kelessis, A.; Paschalidou, A.; Petrakakis, M. Identification of sources and processes affecting particulate pollution in Thessaloniki, Greece. *Atmos. Environ.* **2011**, *45*, 7293–7300. [CrossRef]
59. Giannaros, T.M.; Melas, D. Study of the urban heat island in a coastal Mediterranean City: The case study of Thessaloniki, Greece. *Atmos. Res.* **2012**, *118*, 103–120. [CrossRef]